Rev. Roum. Sci. Techn.– Électrotechn. et Énerg.
Vol. **71**, *4*, pp. 561–566, Bucarest, 2026

ROBOTIC PERCEPTION OF SURFACE TEXTURE THROUGH PSYCHOPHYSICAL TACTILE MODELING

ABDUL ATTAYYAB KHAN[1], BASIT ALI*[1], KANIZ FATIMA[2]

Keywords: Multiresolution sensation; Haptics; Tactile sensing; Robot perception; Low-power sensor.

This paper investigates the use of psychophysical principles for representing tactile information in robotic systems. Although tactile sensing and surface characterization have been extensively studied, representing tactile information from a psychophysical perspective remains an important research question. The work examines whether the sensation associated with rubbing an object can be represented in a robotic tactile system using principles of psychophysical evaluation. This work proposes a psychophysically motivated tactile representation that characterizes relative changes in tactile stimuli across multiple temporal-frequency scales. The tactile response is represented across multiple temporal-frequency bands, and its behavior under slowly varying multiplicative noise is analytically examined. Under the assumptions of the proposed formulation, the analysis indicates that such noise primarily affects the corresponding frequency scale. We evaluate the proposed representation using data from different tactile sensors and experimental platforms to assess its ability to discriminate between materials and surfaces. The proposed representation operates at an abstract perceptual level, aiming to reduce the influence of sensor-specific characteristics on tactile surface information.

1. INTRODUCTION

The quantification of human sensory experience is the central theme of psychophysics [1]. Dating back to two German psychologists of the 19th century [2,3], psychophysics explores the relationship between physical stimuli and their sensations. Let ΔF represent the smallest or "just noticeable difference" (JND) required for a stimulus of magnitude F to be perceived by a subject. "Weber's law", proposed by [3], states that the magnitude of this smallest perception bears a constant relationship with the original magnitude of the stimulus, *i.e.*,

$$k = \frac{\Delta F}{F}, \tag{1}$$

where k is a constant representing weber's ratio. This formulation of sensation has been studied extensively in human vision [4,5], auditory perception [6,7], and the sense of touch [8,9]. Consequently, Weber's perception has been translated into computer vision [10], music [11], and haptics [12].

Weber's law assumes stimuli to be homogeneous [1]. This assumption is rather strict to follow in human perception. In other words, the discrimination between two stimuli is dependent upon the spatial and temporal configuration in which the two are presented for comparison [13]. This motivated [5] to present a band-limited definition of perception in which the visual sensory experience is evaluated locally at different spatial frequency bands. Even though Peli's interpretation is specific to human vision, [13,1] observations hold at an abstract level of perception. Following this observation, we consider whether the relative-response principle underlying Weber's law can be extended to tactile sensing by evaluating tactile stimuli at different temporal-frequency scales. In this view, tactile perception is modeled in a multi-resolution sense, taking into account the human perception of surfaces along different temporal-frequency bands. The perceptual response is then aggregated across these bands to formulate a unified sensory description.

Robots can be designed for a variety of haptic tasks, including manipulation and grasping, assessment of weight and stability, and detection and reaction to contacts from external agents [14]. Tactile perception is particularly important when robots interact physically with their environment, since surface characteristics such as texture, friction, and hardness can influence manipulation and contact behavior. Assessment of the surface relies heavily on automated methods to detect variation in texture and irregularities. Alayat [15] approach can be taken as an example, which analyzes pavement surface conditions through image-based crack detection. These approaches underline the wider relevance of automated surface evaluation, which extends to robotic sensing of texture and influences how robots perceive, act, and communicate with dynamic environments [16]. Moreover, tactile perception, which is essential for contact force estimation and manipulation, helps to improve real-world dynamic constraints, which cannot be deduced from joint measurements alone [17]. In this study, however, we are specifically interested in describing the exploratory behavior of a robot in relation to the physical characteristics of a surface, such as texture, friction, and hardness. These physical characteristics can play an important role in the functional performance of components. Othman [18] demonstrated that surface texture influences surface finish, further highlighting the importance of characterizing surface properties through tactile exploration. More specifically, we seek a feature space that provides a suitable mapping between these objective surface characteristics and their perceptual representation in robotic tactile sensing.

Recent advancements in nanotechnology have enabled robotic sensors to approach the spatial and temporal resolution of a human finger [19]. A human hand can serve as a model for developing tactile sensors such as Polyvinylidene fluoride (PVDF), which mimics the piezoelectric and pyroelectric responses of human skin [20], [21]. Brown [22] defined features as "application- and viewer-dependent interpretations of geometry," suggesting that feature descriptions consider the characteristics of both the sensor and the object being sensed. Okamura [23] formulated surface features using differential geometry by assuming a round robotic finger sliding or rolling over the surface of an object. The authors defined two sets of features, namely curvature and macro features, within the context of haptic exploration. Jia [24] estimated the 2D curvature of an object by placing a manipulator on the object during a rolling motion and established the completeness and local convergence of the model. Shikida [25] used an array of

[1] Department of Electrical Engineering, Bahria University Karachi Campus,13th National Stadium Road, Karachi, Pakistan.
[2] Department of Humanities and Social Sciences, Bahria University Karachi Campus,13th National Stadium Road, Karachi, Pakistan.
E-mails: aakhan.bukc@bahria.edu.pk (corresponding author), basitali.bukc@bahria.edu.pk, Kanifatima.bukc@bahria.edu.pk

DOI: 10.59277/RRST-EE.2026.4.14

sensors to estimate the 2D contact-force distribution, hardness distribution, and surface texture of the perceived object. Gorges [26] utilized moments to compute the position, area, and eccentricity of a contact, as well as principal component analysis (PCA) to identify a low-dimensional subspace for tactile contact patterns. The eigenbasis obtained from PCA decomposition of the covariance matrix of tactile sensor pressure values has also been used as a geometric representation of the surface [27]. The use of two-dimensional sensor arrays further allows descriptors developed in computer vision to be applied to tactile sensing [28]. For instance, Pezzementi [29] used a two-dimensional tactile sensor array to extract scale-invariant feature transform (SIFT)-like responses from surfaces [30]. Statistical features of the sensory input and its frequency distribution have also been used to characterize different fabrics and materials [31,32].

The research mentioned above indicates that tactile surface information can be characterized by geometric, spatial, statistical, and frequency-domain descriptors. However, these approaches primarily characterize the measured sensor response through features associated with the sensing modality and acquisition process, rather than explicitly formulating the representation from a psychophysical perspective. Thus, the choice of sensory feature representation can affect how surface characteristics are represented and discriminated in robotic tactile perception.

There are various tactile descriptors, but an important question is whether surface information can be represented at an intermediate perceptual level inspired by human tactile perception. In particular, relative response to a tactile stimulus and its change across temporal-frequency scales provide a potential basis for developing such a representation.

In this work, we investigate a psychophysically motivated representation of tactile surface information based on the relative-response principle of Weber's law. The tactile signal is processed at various temporal-frequency scales, and the scale-dependent responses are normalized and combined into a single feature representation. This formulation is not intended to propose a new wavelet transform or classification algorithm, but to study whether a perceptual representation based on psychophysical principles could provide a consistent description of tactile surface features in different sensing conditions.

The main contributions of this work are: First, a psychophysically motivated tactile representation is developed. Relative changes in tactile stimuli across multiple temporal-frequency scales are represented using a Weber-like formulation for tactile surface perception. Second, a multi-resolution tactile descriptor is developed based on undecimated wavelet decomposition to obtain scale-dependent tactile responses, which are then normalized and represented as scale-wise histograms to build a compact feature representation. Third, the noise robustness of the proposed representation is analytically investigated under slowly varying multiplicative noise, demonstrating its approximate insensitivity under the assumptions described in the proposed formulation. Finally, the proposed representation is tested across different sensing configurations and acquisition conditions and compared with conventional statistical and frequency-domain descriptors within a common classification framework.

2. PROPOSED SCHEME

The goal of this study is to formulate a feature vector that can capture a Weber-like multi-resolution perception from surfaces. This perception basically measures the magnitude of the change in stimulus relative to its background. Since what constitutes a "background" depends upon a particular scale of analysis, consequently, the perception should also be formulated at different scales. Perhaps the best formulation of perception varying along different scales is presented by [5], where the sensation at a specific scale is defined as the ratio of the band-pass-filtered response of a stimulus at that frequency to its low-pass response filtered at an octave below the same frequency. Following [5] interpretation, we decompose a stimulus f acquired at time t into J temporal-frequency bands and describe the sensation ζ' corresponding to J^{th} band at time t as follows,

$$\zeta'_j(t) = \frac{f_{j-1}(t) - f_j(t)}{f_j(t)}, \quad \exists j \in J, \tag{2}$$

where $f_{j-1}(t) - f_j(t)$ represents the noticeable difference required to perceive the stimulus $f(t)$ at j^{th} scale, while $f_j(t)$ represents the average intensity of $f(t)$ at j^{th} scale. What follows is a way of decomposing f into multiple temporal frequency bands.

A. *Temporal Frequency Decomposition*

We use the undecimated wavelet transform (UWT) [33] to represent an instantaneous stimulus $f(t)$ at different frequency scales. The UWT follows a pyramid-like decomposition where different low- and high-pass representations of $f(t)$ are formulated using a smoothing/wavelet function.

The stimulus f is normalized such that $f \in [0,1]$. Given a mother wavelet, Ψ, a set of low-pass filters can be constructed such that

$$h_j = h_{j-1} \uparrow 2,$$
$$f_j(t) = f_{j-1}(t) h_j, \tag{3}$$

For initialization, $h_1 = \Psi$ and $f_0 = f$. A possible choice for a low-pass cubic spline Ψ is $[0.0625\ 0.25\ 0.375\ 0.25\ 0.0625]$. Let $\Delta f_j(t)$ represent the minimum perceivable difference at j^{th} scale mentioned in (2), *i.e.*,

$$\Delta f_j(t) = f_{j-1}(t) - f_j(t). \tag{4}$$

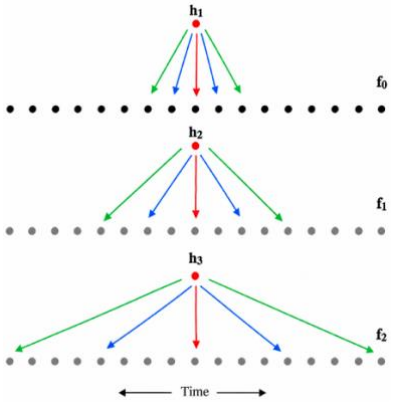

Fig. 1 – UWT decomposition.

The original intensity of the stimulus can be represented as an aggregated response of the minimum perceivable differences approximated at J scales, *i.e.*,

$$f(t) = f_J(t) + \sum_{j=1}^{J} \Delta f_j(t), \tag{5}$$

Figures 2 and 3 present a sample three-stage decomposition.

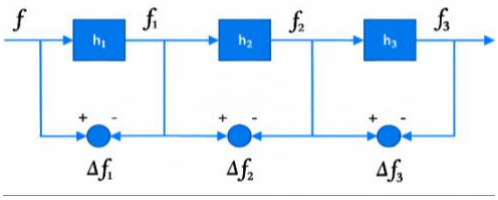

Fig. 2 – Signal decomposition.

B. *Feature Representation*

A simple frequency count of the perceptual responses can act as a feature vector. However, the perception obtained through (2) cannot be directly transformed into a compact histogram representation. A problem with (2) is that it can result in very high values of sensation where the average stimulus appearing in the denominator is very low. To normalize against very low and very high perceptual values, we use a sigmoidal mapping at each scale, *i.e.*,

$$\zeta_j(t) = \left(1 + \exp\left(-\frac{\zeta_j'(t) - \beta}{\alpha}\right)\right)^{-1}, \qquad (6)$$

where β and α represent the mean and standard deviation of ζ_j', respectively. Figures 4 and 5 show an example of an original and a normalized feature vector; $\zeta_j(t) \in [0,1]$ represents a normalized perception of $f(t)$ at j^{th} scale; ζ_j is represented as an N-dimensional histogram, while the histogram representations of J scales are concatenated to form a $N \times J$ dimensional feature vector. One can apply PCA on the $N \times J$ dimensional feature space of a given dataset to visualize the 3D space spanned by the principal components.

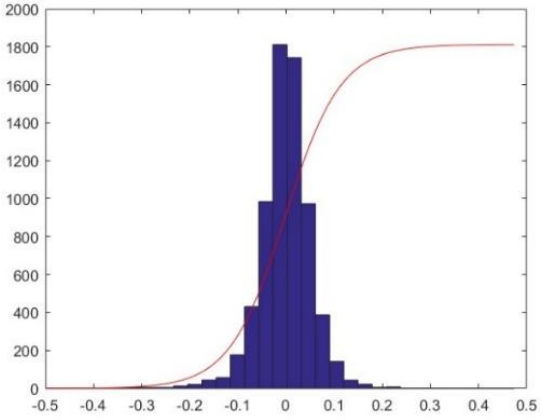

Fig. 4 – A 50-bin histogram resulting from (2) at $j = 1$ (blue) and the corresponding stretching function (red)

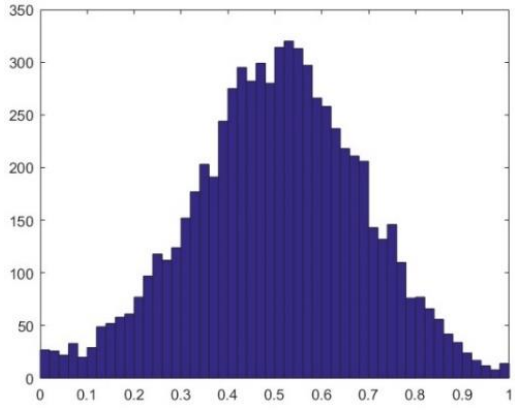

Fig. 5 – Normalized sensation: A 50-dimensional feature vector.

Figure 6 shows the proposed perceptual representation projected onto the first three principal components for 28 surface difference types presented in [32].

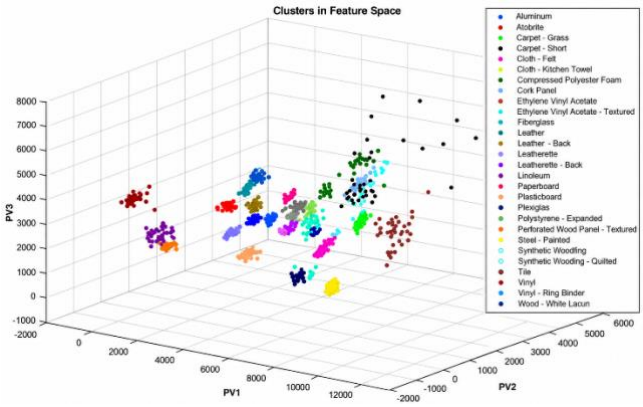

Fig. 6 – Signal Decomposition

C. *Noise Invariance*

By definition, (2) is invariant to linear noise. Let f be corrupted by multiplicative noise n such that

$$\tilde{f}(t) = (f \cdot n)(t), \qquad (7)$$

where f represents the characteristics of the fabric or the material, while $\tilde{f}(t)$ represents the modified stimulus observed by a robot at time t. The sensation obtained at the 1st scale is given by

$$\zeta_1'(t) = \frac{\tilde{f}(t) - \tilde{f}_1(t)}{\tilde{f}_1(t)} = \frac{\big((f \cdot n) - (f \cdot n) \cdot h_1\big)(t)}{\big((f \cdot n) \cdot h_1\big)(t)}. \qquad (8)$$

If the noise varies slowly such that it is constant over the length of h_1 (window length of 5), *i.e.*,

$$\big((f \cdot n) \cdot h_1\big)(t) \approx \big((f \cdot h_1) \cdot n\big)(t), \qquad (9)$$

we can rewrite (8) as,

$$\zeta_1'(t) = \frac{f(t) - (f \cdot h_1)(t)}{(f \cdot h_1)(t)}. \qquad (10)$$

Since n is missing from (10), the sensation measured at the 1st scale is approximately independent of noise and depends solely on the characteristics of the object described by f.

In Fig. 2, observe that f_1 (*i.e.*, the input to the 2nd scale) is a low-pass version of f. Since the variances of n within the window length of h_1 have already been accounted for, it is safe to assume that n will remain constant over the window length of h_2. Similarly, assuming n to be constant within a particular scale, it can easily be shown that the sensation at that scale is approximately independent of the multiplicative noise. In short, we remove the high-frequency effects of noise before passing the input to the coarser scales. Therefore, the effects of noise related to a particular temporal-frequency band do not affect the sensations of adjacent bands.

3. MATERIAL CLASSIFICATION

The histogram representation can be used to categorize different types of materials. We believe that a good representation is one that performs comparatively well even in complex scenarios. Since the focus of this paper is to compare the tactile feature representations rather than to develop or optimize a classification model, a simple nearest-neighbor classifier is used in all experiments. The same classification framework is applied to the proposed

representation and the considered conventional descriptors, allowing their discriminatory capability to be compared under the same evaluation procedure. For each dataset, the selected training samples are used by the nearest-neighbor classifier, while the remaining samples are evaluated as test samples. The classifier simply assigns that label to a given test sample that minimizes the L1 distance across all training samples. Table I summarizes the descriptors chosen for evaluation. Most of these are already used for material classification [34]. Additionally, a concatenated feature set of these 12 features is also used for comparison. The hypothesis that the "feature space is robust against the subjective constraints of the sensor" is tested by classifying materials acquired through different sensors and acquisition protocols.

Table 1
List of features extracted from the sensor signal.

Notation	Length	Description
F_{max}	1	Maximum value of the signal
F_{min}	1	Minimum value of the signal
F_{mean}	1	Mean value of the signal
F_{var}	1	Variance of the signal
F_{norm}	1	L2 Norm of the signal
F_{kurt}	1	Kurtosis coefficient of the signal
F_{skew}	1	Skew of the signal
F_{range}	1	Range of values
F_{mode}	1	Mode of the signal
F_{5th}	1	Fifth Moment of the signal
$F_{H,frq}$	1	Maximum frequency value in the signal
$F_{S,h}$	1	Sum of higher half of the Fourier spectrum
F_{12}	12	Concatenation of above-mentioned features

A. Polyvinylidene Fluoride-Based Sensation

Jamali [31] acquired nine different types of materials by rubbing a biologically inspired artificial finger over the surface. The silicon-made finger mounted on the 9-DOF gripper is embedded with randomly distributed PVDF sensors and strain gauges. The randomly distributed sensors are placed in two different layers. The external layer of the finger, which is harder than the internal layer, reduces the stickiness of the silicon-made finger. The inner part is softer and ensures the conformity of the finger during contact with the object. The whole structure of the finger is supported through a back covering. The data acquisition unit sets the finger temporal resolution at 2.5 kHz. We only consider data acquired using four PVDF sensors. There are 50 samples available for each of nine different types of materials. A subset of these 50 samples is chosen for training, while testing is performed on all the remaining samples. Table 2 presents the classification accuracies on this dataset.

Table 2
Evaluation of descriptors for nine different material types [31].

Notation	Feature Length	No. of training samples		
		1	10	25
F_{max}	4	37.86%	46.83%	48.76%
F_{min}	4	38.37%	45.76%	48.27%
F_{mean}	4	47.56%	65.40%	67.99%
F_{var}	4	56.90%	69.46%	72.92%
F_{norm}	4	62.95%	79.03%	81.48%
F_{kurt}	4	41.66%	54.41%	56.42%
F_{skew}	4	44.45%	61.66%	66.32%
F_{range}	4	40.46%	51.18%	53.07%
F_{mode}	4	15.87%	19.37%	21.60%
F_{5th}	4	42.02%	53.57%	56.68%
$F_{H,frq}$	4	47.56%	65.40%	67.99%
$F_{S,h}$	4	63.62%	77.91%	79.24%
F_{12}	48	77.12%	94.31%	95.79%
Proposed	120	71.85%	87.68%	89.92%

The fewer number of sensor channels results in low dimensionality of statistical features, due to which the features do not perform well independently. This performance improves when a set of concatenated statistical features is used for classification. The proposed sensory representation maintains a decent enough classification accuracy.

B. Sensation through Accelerometers

Accelerometers are the most widely used dynamic tactile sensors. We consider two datasets acquired using three-axis accelerometers.

1) *Tool-Mediated Texture Recognition:*

In [35], both controlled and unconstrained environments are used to capture vibrations over different surfaces. We use data acquired through controlled acquisition wherein 20 examples are acquired for a single class. These 20 samples are acquired either by increasing force or velocity in a linear fashion.

The authors acquired 108 categories, which, to our knowledge, amounts to the largest number of material types acquired so far. We skip the pre-processing stage and use the magnitude of acceleration extracted from the three directional values of acceleration as our single-channel signal input.

Table 3 presents the classification results on this database. Since the data is acquired at 48 kHz, we set J = 5, resulting in an N(bins)×J(scales)=10×5=50-dimensional feature vector. Due to a single-channel acquisition, the low-dimensional statistical features do not work well in this case.

The set of concatenated statistical features improves the performance, but the proposed descriptor outperforms this set by a factor of 3 in terms of average accuracy when 10 samples are used for training.

Table 3
Evaluation of descriptors over LMT 108 dataset [35].

Feature	Feature Length	No. of training samples		
		1	5	10
F_{max}	1	5.02%	6.05%	7.02%
F_{min}	1	1.85%	2.68%	3.68%
F_{mean}	1	5.12%	5.41%	5.57%
F_{var}	1	5.13%	5.04%	5.10%
F_{norm}	1	5.22%	5.25%	4.70%
F_{kurt}	1	2.71%	2.81%	2.90%
F_{skew}	1	3.52%	3.61%	4.02%
F_{range}	1	5.02%	5.56%	5.82%
F_{mode}	1	1.64%	2.37%	3.30%
F_{5th}	1	5.69%	5.90%	6.11%
$F_{H,frq}$	1	5.12%	5.42%	5.57%
$F_{S,h}$	1	4.81%	4.88%	4.74%
F_{12}	12	12.20%	17.95%	20.26%
Proposed	50	26.00%	51.25%	59.78%

2) *Surface Identification:*

A triple-axis accelerometer has been used in [32] to collect 28 types of surfaces. The acquisition on each surface was done for 20 min. We break down this acquisition into segments of 30 ss (time window corresponding to 24000 samples). For each surface, this gives us a minimum of 40 examples, out of which we randomly select a subset for training, while testing is done on all the remaining examples.

The results shown in Table 4 suggest that the proposed descriptor performs consistently well in this dataset.

Table 4

Evaluation of descriptors over 28 surfaces [32].

Feature	Feature Length	No. of training samples		
		1	5	10
F_{max}	1	47.87%	49.25%	49.56%
F_{min}	1	29.19%	31.09%	31.45%
F_{mean}	1	63.09%	67.88%	68.32%
F_{var}	1	71.02%	76.06%	76.66%
F_{norm}	1	57.25%	59.49%	60.66%
F_{kurt}	1	35.44%	36.78%	37.26%
F_{skew}	1	47.71%	50.68%	51.49%
F_{range}	1	47.14%	47.73%	48.46%
F_{mode}	1	14.75%	16.34%	16.63%
F_{5th}	1	68.65%	72.62%	73.68%
$F_{H,frq}$	1	63.09%	67.88%	68.32%
$F_{S,h}$	1	61.55%	64.05%	64.49%
F_{12}	12	94.83%	99.28%	99.68%
Proposed	50	95.49%	99.75%	99.91%

4. **CONCLUSIONS**

This paper investigates the psychophysical perception of tactile sensing. A psychophysically motivated tactile descriptor is proposed based on a Weber-like response across multiple temporal-frequency scales. The resulting description captures tactile responses at different frequency scales and is aggregated into a unified representation. The effect of slowly varying multiplicative noise within a particular scale is confined to that scale and does not affect the descriptions of adjacent scales under the assumptions of the proposed formulation. The resulting descriptor is transformed into a feature vector by counting the number of occurrences of a particular stimulus. The resulting feature space is used to categorize different materials and surfaces. This categorization is evaluated using data acquired from different tactile sensors and experimental platforms, demonstrating the discriminative capability of the proposed representation across the evaluated acquisition protocols.

CREDIT AUTHORSHIP CONTRIBUTION

Abdul Attayyab KHAN: Conceptualization; modeling; literature review.

Basit ALI: Writing, methodology.

Kaniz FATIMA: Mathematical formulation; references; language correction.

Received on 6 March 2026

REFERENCES

1. L.L. Thurstone, "Psychophysical analysis," American Journal of Psychology, **38**, *3*, pp. 368–389 (1927).
2. E. Weber, "Über den Tastsinn," Archiv für Anatomie, Physiologie und Wissenschaftliche Medicin (Berlin), **1**, pp. 152–159 (1835).
3. G.T. Fechner, "Elemente der Psychophysik," vol. 2, Breitkopf und Härtel, Leipzig (1860).
4. G.E. Legge, "A power law for contrast discrimination," Vision Research, **21**, *4*, pp. 457–467 (1981).
5. E. Peli, "Contrast in complex images," Journal of the Optical Society of America A, **7**, *10*, pp. 2032–2040 (1990).
6. R. Riesz, "Differential intensity sensitivity of the ear for pure tones," Physical Review, **31**, *5*, p. 867 (1928).
7. W.J. McGill, "Neural counting mechanisms and energy detection in audition," J. of Mathematical Psychology, **4**, *3*, pp. 351–376 (1967).
8. A.B. Vallbo, R.S. Johansson, "Properties of cutaneous mechanoreceptors in the human hand related to touch sensation," Human Neurobiology, **3**, *1*, pp. 3–14 (1984).
9. M.A. Heller, W. Schiff, "Conclusions: The future of touch," in The psychology of touch, Psychology Press, pp. 327–337 (2013), ISBN 0-8058-0750-0, ISBN 0-8058-0751-9.
10. J. Chen, et al., "WLD: A robust local image descriptor," IEEE Transactions on Pattern Analysis and Machine Intelligence, **32**, *9*, pp. 1705–1720 (2009).
11. E. Gunther, S. O'Modhrain, "Cutaneous grooves: Composing for the sense of touch," Journal of New Music Research, **32**, *4*, pp. 369–381 (2003).
12. S. Feyzabadi, S. Straube, M. Folgheraiter, E.A. Kirchner, S.K. Kim, J.C. Albiez, "Human force discrimination during active arm motion for force feedback design," IEEE Transactions on Haptics, **6**, *3*, pp. 309–319 (2013).
13. D. Laming, "Sensory analysis," Academic Press, London (1986).
14. M.R. Cutkosky, R.D. Howe, W.R. Provancher, "Force and tactile sensors," in Springer Handbook of Robotics, pp. 455–476 (2008).
15. A.B. Alayat, H.A. Omar, "Pavement surface distress detection using digital image processing techniques," J. Kejuruter, **35**, *1*, pp. 247–256 (2023).
16. M. El Mesbahi, A. Tgarguifa, H. Hachimi, "Robot morphologies and communication strategies trade-off in a dynamic multi-robot collaborative environment," Rev. Roum. Sci. Techn. – Électrotechn. Et Énerg., **67**, *2*, pp. 193–198 (2022).
17. W. Han, H. Qin, "A velocity self-learning algorithm for time-optimal trajectory planning along fully specified path – Part II," Rev. Roum. Sci. Techn. – Électrotechn. Et Énerg., **70**, *2*, p. 241 (2025).
18. T. Othman, H.A. Rahman, J.A. Ghani, C.H.C. Haron, "Surface roughness in high-speed turning of alloy steel M303 using carbide tools in dry cutting condition," J. Kejuruter., **34**, *6*, pp. 1169–1173 (2022).
19. V. Maheshwari, R.F. Saraf, "High-resolution thin-film device to sense texture by touch," Science, **312**, *5779*, pp. 1501–1504 (2006).
20. J. Dargahi, S. Najarian, "Human tactile perception as a standard for artificial tactile sensing—a review," International Journal of Medical Robotics and Computer Assisted Surgery, **1**, *1*, pp. 23–35 (2004).
21. R.S. Dahiya, G. Metta, M. Valle, G. Sandini, "Tactile sensing—from humans to humanoids," IEEE Transactions on Robotics, **26**, *1*, pp. 1–20 (2010).
22. K.N. Brown, C.A. McMahon, J.H.S. Williams, "Features, aka the semantics of a formal language of manufacturing," Research in Engineering Design, **7**, *3*, pp. 151–172 (2025).
23. A.M. Okamura, M.R. Cutkosky, "Feature detection for haptic exploration with robotic fingers," International Journal of Robotics Research, **20**, *12*, pp. 925–938 (2001).
24. Y.-B. Jia, "Localization of curved parts through continual touch," IEEE Transactions on Robotics, **21**, *4*, pp. 726–733 (2005).
25. M. Shikida, T. Shimizu, K. Sato, K. Itoigawa, "Active tactile sensor for detecting contact force and hardness of an object," Sensors and Actuators A: Physical, **103**, *1–2*, pp. 213–218 (2003).
26. N. Gorges, S.E. Navarro, D. Göger, H. Wörn, "Haptic object recognition using passive joints and haptic key features," in 2010 IEEE International Conference on Robotics and Automation (ICRA), IEEE, pp. 2349–2354 (2010).
27. J. Bimbo, S. Luo, K. Althoefer, H. Liu, "In-hand object pose estimation using covariance-based tactile to geometry matching," IEEE Robotics and Automation Letters, **1**, *1*, pp. 570–577 (2016).
28. S. Luo, W.D. Mou, K. Althoefer, H. Liu, "Novel Tactile-SIFT descriptor for object shape recognition," IEEE Sensors Journal, **15**, *9*, pp. 5001–5009 (2015).
29. Z. Pezzementi, E. Plaku, C. Reyda, G.D. Hager, "Tactile-object recognition from appearance information," IEEE Transactions on Robotics, **27**, *3*, pp. 473–487 (2011).
30. J. Zhang, M. Marszalek, S. Lazebnik, C. Schmid, "Local features and kernels for classification of texture and object categories: A comprehensive study," in 2006 IEEE Computer Society Conference on Computer Vision and Pattern Recognition – Workshops (CVPRW), IEEE, p. 121 (2006).
31. N. Jamali, C. Sammut, "Majority voting: Material classification by tactile sensing using surface texture," IEEE Transactions on Robotics, **27**, *3*, pp. 508–521 (2011).
32. P. Dallaire, D. Emond, P. Giguere, B. Chaib-Draa, "Artificial tactile perception for surface identification using a triple axis accelerometer probe," in 2011 IEEE International Symposium on Robotic and Sensors Environments (ROSE), IEEE, pp. 101–106 (2011).
33. J.-L. Starck, J. Fadili, F. Murtagh, "The undecimated wavelet decomposition and its reconstruction," IEEE Transactions on Image Processing, **16**, *2*, pp. 297–309 (2007).
34. C. Weiss, H. Fröhlich, A. Zell, "Vibration-based terrain classification using support vector machines," in 2006 IEEE/RSJ International Conference on Intelligent Robots and Systems (IROS), IEEE, pp. 1429–1434 (2006).
35. M. Strese, J.-Y. Lee, C. Schuwerk, Q. Han, H.-G. Kim, E.G. Steinbach, "A haptic texture database for tool-mediated texture recognition and classification," in 2014 IEEE International Symposium on Haptic, Audio and Visual Environments and Games (HAVE), IEEE, pp. 118–123 (2014).
36. M. Strese, J.-Y. Lee, C. Schuwerk, Q. Han, H.-G. Kim, E.G. Steinbach, "A haptic texture database for tool-mediated texture recognition and classification," in 2014 IEEE International Symposium on Haptic, Audio and Visual Environments and Games (HAVE), IEEE, pp. 118–123 (2014).